ELSEVIER

Coordination Chemistry Reviews
216–217 (2001) 513–536

COORDINATION CHEMISTRY REVIEWS

www.elsevier.com/locate/ccr

Shape- and enantioselective interaction of Ru(II)/Co(III) polypyridyl complexes with DNA

Liang-Nian Ji *, Xiao-Hua Zou, Jin-Gang Liu

State Key Laboratory of Ultrafast Laser Spectroscopy/Department of Chemistry, Zhongshan University, Guangzhou 510275, People's Republic of China

Received 8 August 2000; received in revised form 10 January 2001; accepted 22 January 2001

Contents

Abstract . . . 514
1. Introduction . . . 514
2. Shape selective interaction with DNA . . . 515
   2.1 Planarity of the intercalative ligand . . . 515
      2.1.1 Effect of the planarity on the binding geometry . . . 515
      2.1.2 Effect of the planarity on binding affinity . . . 516
   2.2 Ancillary ligands . . . 517
   2.3 Probing the shape selective interaction of Co(III) complexes with DNA . . . 519
3. Enantioselective binding to DNA . . . 522
   3.1 Electronic absorption spectra . . . 522
   3.2 Steady-state emission titration . . . 523
   3.3 Viscosity measurements . . . 525
   3.4 Equilibrium dialysis . . . 526
4. The further development of a molecular light switch for DNA . . . 529
   4.1 The design of novel molecular light switches for DNA . . . 529
   4.2 Possible mechanism of the light switch effect for DNA . . . 532
Acknowledgements . . . 533
Appendices . . . 533
References . . . 535

* Corresponding author. Tel.: +86-20-8411-0115; fax: +86-20-8403-5497.
E-mail address: cesjln@zsu.edu.cn (L.-N. Ji).

PII: S0010-8545(01)00338-1

Abstract

This paper presents recent progress in our laboratory on the interaction of Ru(II)/Co(III) polypyridine complexes with DNA. The first part describes the effect on DNA binding of modulating the intercalative ligand and the size of the ancillary ligand of the complex. DNA binding modes and binding affinity can be modulated by ligand design. The second part focuses on the enantioselective DNA binding behavior of the Ru(II) complexes using absorption spectra, emission spectra, viscosity measurements, equilibrium dialysis and CD titrations. The enantiomers of the various Ru(II) complexes show diverse enantioselectivity on binding to DNA. Different equilibrium rates were observed for the enantiomers of the complex in a time-dependent dialysis experiment. The interesting effect of the "molecular switch" for DNA was observed for several Ru(II) complexes. Their DNA binding properties, together with the possible mechanism involved in the effect, are discussed in the last part.

Keywords: Ru(II) complexes; Co(III) complexes; Polypyridine; DNA; Enantioselectivity; Light switch

1. Introduction

In recent years, transition metal complexes have been used extensively in the forefront of fields such as probes of DNA structure, DNA-dependent electron transfer and DNA site specific cleavage [1–3]. These efforts stem from the search for an understanding of drug–nucleic acid interactions on a molecular level and from the development of novel chemotherapeutics and highly sensitive diagnostic agents.

Stable, inert and water-soluble octahedral complexes containing spectroscopically active metal centers are found to be valuable in the above applications. Octahedral complexes provide useful and sensitive tools for probing DNA structure with site specificity because the complexes can be modified and functionalized in three dimensions to adapt the helix. In this case the shape of the complex plays a key role in the interaction with DNA [4]. Moreover, the octahedral complexes were found to interact with DNA enantioselectively and the right-handed Δ-isomer was favored on intercalation to right-handed B-DNA [5]. It is noteworthy that the model was first proposed for $[Ru(phen)_3]^{2+}$. However, the binding nature of $[Ru(phen)_3]^{2+}$ with DNA remains an issue of vigorous debate [6–15]. In fact the left-handed Λ-isomer of the octahedral complex has been reported to show preference upon binding to right-handed DNA under some conditions [16–18]. Therefore the factors governing the enantioselectivity on binding to DNA for octahedral complexes can be further elucidated with more detailed studies as will be reported in this paper.

2. Shape selective interaction with DNA

2.1. Planarity of the intercalative ligand

2.1.1. Effect of the planarity on the binding geometry

Generally the intercalative ligand should contain an aromatic heterocyclic functionality that can insert and stack between the base pairs of double helical DNA [19]. However, octahedral complexes with the non-planar ligand 4,7-diphenyl-1,10-phenanthroline (DIP) $[Ru(DIP)_3]^{2+}$ [4,20,21] and quaterpyridine (qpy) $[Ru(bpy)_2(qpy)]^{2+}$ [16] were found to be bound to DNA in an intercalation mode. So it is interesting to find the effect of the non-planarity of the ligand on intercalation and on the binding affinity and binding geometry of the complex with DNA. Indeed the DNA binding study on the complexes containing the planar ligand 2-phenyl-imidazo[4,5-f]1,10-phenanthroline (pip) $[Ru(bpy)_2(pip)]^{2+}$ [22] and the non-planar ligand 2-(2-chloro-phenyl-)imidazo[4,5-f]1,10-phenanthroline (CIP) $[Ru(bpy)_2(CIP)]^{2+}$ [23] indicate that these two complexes intercalate into DNA base pairs with different binding geometry.

The absorption spectrum of $[Ru(bpy)_2(pip)]^{2+}$ showed significant perturbation on addition of CT-DNA, with hypochromism of about 22% in the metal to ligand charge transfer (MLCT) band as shown in Table 1. However, upon inclusion of a substituent Cl at the 2-position in the phenyl ring, the hypochromism of the MLCT band for $[Ru(bpy)_2(CIP)]^{2+}$ decreased by 10%. The results of emission titrations for $[Ru(bpy)_2(pip)]^{2+}$ and $[Ru(bpy)_2(CIP)]^{2+}$ indicate that the magnitudes of emission enhancement for the latter are much smaller than that of the former. Since emission enhancement and lifetime increase are related to the extent to which the complex gets into a hydrophobic environment inside the DNA and avoids the quenching effect of solvent water molecules, the above results imply that $[Ru(bpy)_2(CIP)]^{2+}$ inserts less deeply into the hydrophobic environment of DNA than does $[Ru(bpy)_2(pip)]^{2+}$. Steady emission quenching experiments using the anionic $[Fe(CN)_6]^{4-}$ as the quencher support the above proposal. In the absence of DNA, both $[Ru(bpy)_2(pip)]^{2+}$ and $[Ru(bpy)_2(CIP)]^{2+}$ were efficiently quenched by $[Fe(CN)_6]^4$, resulting in a linear Stern–Volmer plot. The Stern–Volmer quenching constant (K_{SV}) for the two complexes was similar (2.2×10^3 M^{-1}). However, although the plots for both $[Ru(bpy)_2(pip)]^{2+}$ and $[Ru(bpy)_2(CIP)]^{2+}$ were curved in the presence of DNA, K_{SV} for the latter (8.9×10^2 M^{-1}) [23] is much larger than

Table 1
Spectroscopic properties of $[Ru(bpy)_2(pip)]^{2+}$ and $[Ru(bpy)_2(CIP)]^{2+}$ on binding to DNA

Complex	Absorption		Emission		
	λ_{max} (nm)	Hypochromism (%)	λ_{max} (nm)	I/I_0	τ/τ_0
$[Ru(bpy)_2(pip)]^{2+}$	458	22	615	2.6	3.5
$[Ru(bpy)_2(CIP)]^{2+}$	457	12	611	1.9	2.1

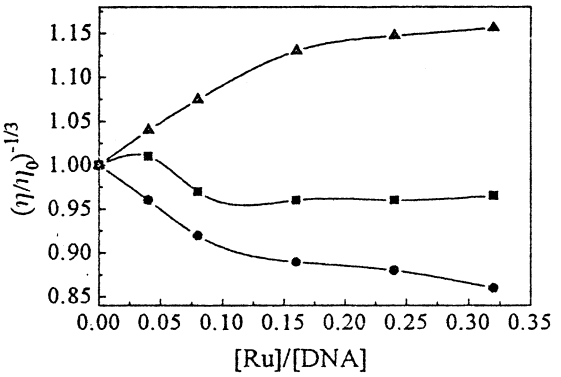

Fig. 1. Effect of increasing amounts of $[Ru(bpy)_2(pip)]^{2+}$ (▲), $[Ru(bpy)_2(CIP)]^{2+}$ (■) and $[Ru(bpy)_2(CIP)]^{2+}$ (●) on the relative viscosity of calf thymus DNA [23]. Reproduced from ref. [23] with permission of The Royal Society of Chemistry.

the former (1.5×10^2 M^{-1}) [22]. The much larger K_{SV} for $[Ru(bpy)_2(CIP)]^{2+}$ in the presence of DNA reflects that the complex is more efficiently quenched by $[Fe(CN)_6]^{4-}$ and is less protected by DNA [24].

The more interesting observation may be from viscosity measurements (Fig. 1). It can be clearly seen that $[Ru(bpy)_2(pip)]^{2+}$ and $[Ru(bpy)_2(CIP)]^{2+}$ produce contrasting effects on DNA viscosity, $[Ru(bpy)_2(pip)]^{2+}$ increases the viscosity in a similar fashion to the proven DNA intercalator $[Ru(bpy)_2(dppz)]^{2+}$, [25] but $[Ru(bpy)_2(CIP)]^{2+}$ and $[Ru(bpy)_2(NIP)]^{2+}$ (NIP = 2-(2-nitrophenyl-)imidazo[4,5-f]1,10-phenanthroline) decreasing it as the molar ratio of Ru(II) complex to DNA was increased, similar to the observation for Δ-$[Ru(phen)_3]^{2+}$ [10,11]. A classical intercalation model demands that the DNA helix lengthen as base pairs are separated to accommodate the bound ligand, leading to an increase of DNA viscosity. In contrast, a partial, non-classical intercalation of ligand could bend (or kink) the DNA helix, reduce its effective length and, concomitantly, its viscosity [10]. The experimental results suggest that $[Ru(bpy)_2(CIP)]^{2+}$ may bind to DNA by a non-classical, partial intercalation mode. This may be related to the large torsion angle (44.5°) in the ligand CIP between the phenyl ring and the fused imidazo moiety as indicated by the crystal structure of the complex (Fig. 2) [23]. Because of the steric constraint to the co-planarity of the phenyl containing a large substituent Cl and the ip moiety in CIP, the complex could only partially penetrate their substituted phenyl moiety into the DNA base pairs, prying apart one side of a base pair stack and causing a static bend or kink in the helix, and decrease the viscosity of DNA.

2.1.2. Effect of the planarity on binding affinity

It is expected that increasing the surface area for intercalative stacking by a complex leads to a substantially increased intercalative binding affinity [26]. However, if the increased part is non-planar relative to the parent ligand, the binding

affinity may be decreased as observed for $[Ru(bpy)_2(taptp)]^{2+}$ and $[Ru(bpy)_2(dptatp)]^{2+}$ [27].

Addition of CT-DNA produced a more significant perturbation on the absorption spectrum of $[Ru(bpy)_2(taptp)]^{2+}$ than on $[Ru(bpy)_2(dptatp)]^{2+}$. For $[Ru(bpy)_2(taptp)]^{2+}$ a red shift of 8 nm and hypochromism of 24% were observed in the intraligand (IL) energy band on binding to DNA while $[Ru(bpy)_2(dptatp)]^{2+}$ displays hypochromism of 13% in both the IL and MLCT bands and a red shift of 9 nm in the IL band. The intrinsic binding constant K_b was determined as 1.7×10^5 M^{-1} for $[Ru(bpy)_2(taptp)]^{2+}$ and 3.8×10^4 M^{-1} for $[Ru(bpy)_2(dptatp)]^{2+}$ using the MLCT absorption [4]. The results of emission titrations for the two complexes are shown in Fig. 3 and the difference is much larger than that observed in the absorption spectra. The ratios of the emission intensity at saturated DNA concentration to the original intensity are 15 and 3 for $[Ru(bpy)_2(taptp)]^{2+}$ and $[Ru(bpy)_2(dptatp)]^{2+}$, respectively. The great difference in emission titrations is consistent with the proposal that $[Ru(bpy)_2(taptp)]^{2+}$ binds more avidly to DNA than does $[Ru(bpy)_2(dptatp)]^{2+}$. The results of emission quenching of the two complexes with increasing concentrations of $[Fe(CN)_6]^{4-}$ (Fig. 4) indicate that $[Ru(bpy)_2(dptatp)]^{2+}$ was quenched more efficiently than $[Ru(bpy)_2(taptp)]^{2+}$, and support the above proposal that the latter has a higher DNA binding affinity. This significant difference in DNA binding affinity can be rationalized in terms of the fully aromatic planarity of the ligand taptp in $[Ru(bpy)_2(taptp)]^{2+}$ and the non-planarity of the ligand dptatp in $[Ru(bpy)_2(dptatp)]^{2+}$. It is expected that the non-planarity of the ligand dptatp originates from the hydrogen atom interaction of the two phenyl groups. Therefore $[Ru(bpy)_2(dptatp)]^{2+}$ fits more poorly to the DNA helical structure relative to $[Ru(bpy)_2(taptp)]^{2+}$ and binds to DNA less strongly.

2.2. Ancillary ligands

Since the octahedral complex binds to DNA in three dimensions, its ancillary ligand can also be modified or functionalized to tune the DNA binding property.

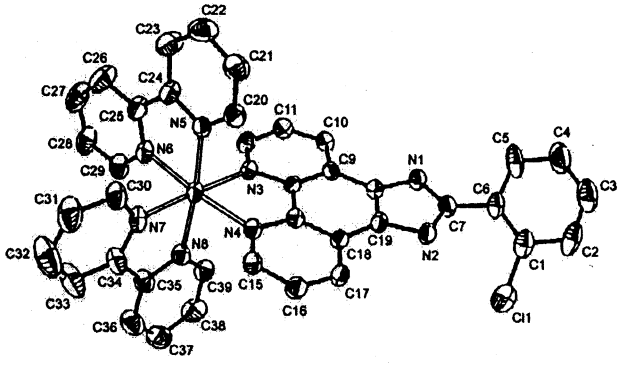

Fig. 2. An ORTEP drawing of $[Ru(bpy)_2(CIP)]^{2+}$ [23]. Reproduced from ref. [23] with permission of The Royal Society of Chemistry.

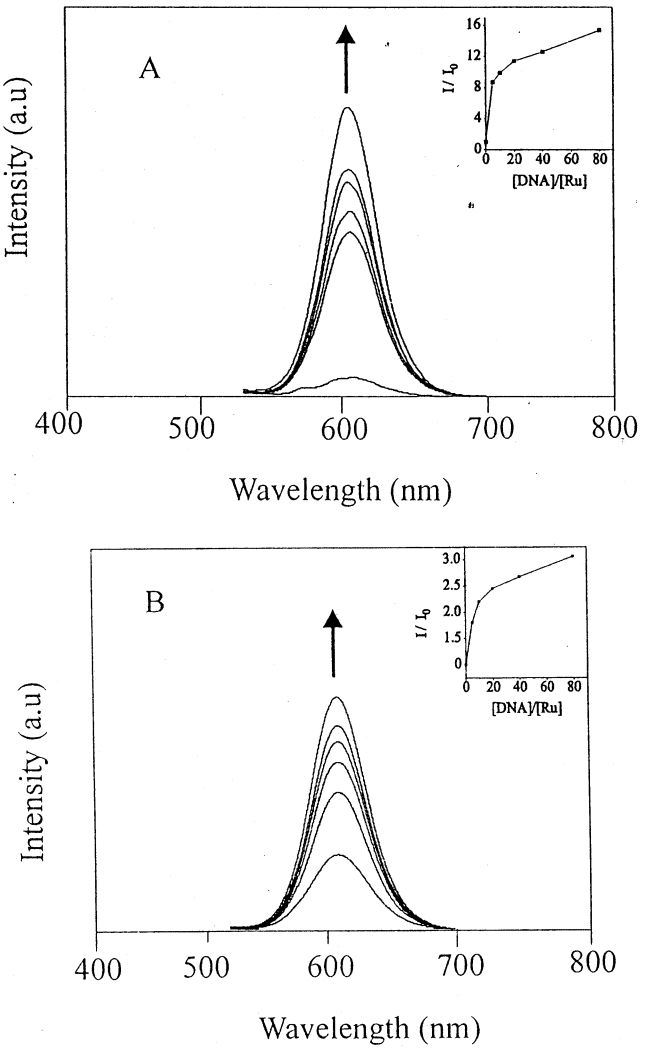

Fig. 3. Emission spectra of: (A) $[Ru(bpy)_2(taptp)]^{2+}$; and (B) $[Ru(bpy)_2(dptatp)]^{2+}$ in aqueous buffer (5 mM Tris, 50 mM NaCl, pH 7.0, [Ru] = 2 M) at 298 K in the presence of 0, 10, 20, 40, 80 and 160 M calf thymus DNA. Arrows show the emission changes upon increasing DNA concentration. Inset: plots of relative integrated emission intensity [27]. Reproduced from ref. [27] with permission of Elsevier Science.

As has been documented before, if the ancillary ligand is tethered with bulky and non-aromatic groups such as $-CH_3$, the DNA binding of the complex will be greatly weakened [28]. However, increasing the surface area of the ancillary ligand may increase the DNA binding affinity of the complex, as exhibited by $[Ru(ip)_2(dppz)]^{2+}$ [29].

The changes in the absorption spectrum of $[Ru(ip)_2(dppz)]^{2+}$ in the visible region with increasing amounts of DNA are shown in Fig. 5. It is very interesting that the

IL band at 372 nm (attributed to the intraligand π–π* transition of dppz) and the MLCT band at 454 nm show pronounced hypochromism of 46 and 40%, respectively. This observation is different from what is observed for $[Ru(bpy)_2(dppz)]^{2+}$, [30] whose IL and MLCT bands were decreased by 39 and 12%. The binding constant K was calculated as 2.1×10^7 M^{-1} for $[Ru(ip)_2(dppz)]^{2+}$, which is somewhat higher than that for $[Ru(bpy)_2(dppz)]^{2+}$ (4.9×10^6 M^{-1}) under similar conditions [29] The binding constant for $[Ru(bpy)_2(dppz)]^{2+}$ is similar to that obtained by others [31,32]. $[Ru(ip)_2(dppz)]^{2+}$ showed weak luminescence in Tris buffer in the absence of CT-DNA. On addition of the DNA, the emission intensity of the complex was enhanced appreciably, with the emission maximum shifting from 604 to 617 nm. The absorption spectra, together with the emission behavior indicate that the DNA binding affinity of $[Ru(ip)_2(dppz)]^{2+}$ was increased with a more extended surface area ancillary ligand relative to $[Ru(bpy)_2(dppz)]^{2+}$.

2.3. Probing the shape selective interaction of Co(III) complexes with DNA

During studies on the interaction of transition metal complexes with DNA, little attention has been paid to Co(III) complexes [8,20,33–35]. In fact, with a redox-ac-

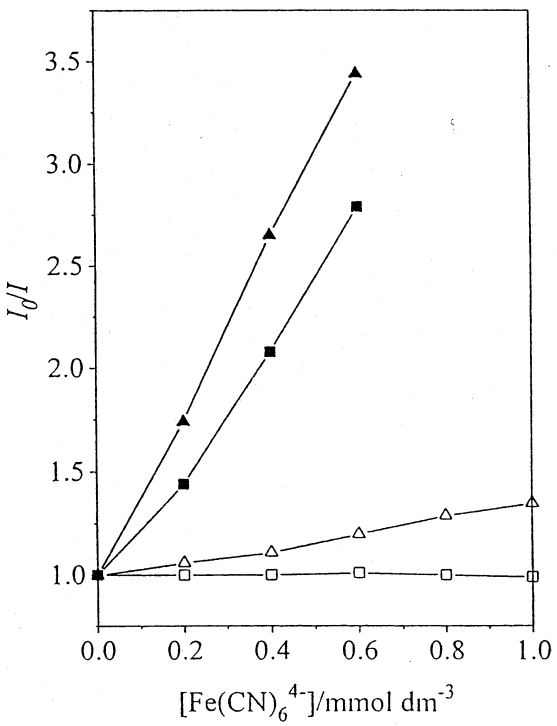

Fig. 4. Emission quenching of $[Ru(bpy)_2(taptp)]^{2+}$ and $[Ru(bpy)_2(dptatp)]^{2+}$ with increasing concentrations of $[Fe(CN)_6]^{4-}$. [Ru] = 2 μM, [DNA]/[Ru] = 40:1. Free $[Ru(bpy)_2(dptatp)]^{2+}$ (▲), $[Ru(bpy)_2(taptp)]^{2+}$ (■), $[Ru(bpy)_2(dptatp)]^{2+}$ + DNA (Δ), $[Ru(bpy)_2(taptp)]^{2+}$ + DNA (□) [27]. Reproduced from ref. [27] with permission of Elsevier Science.

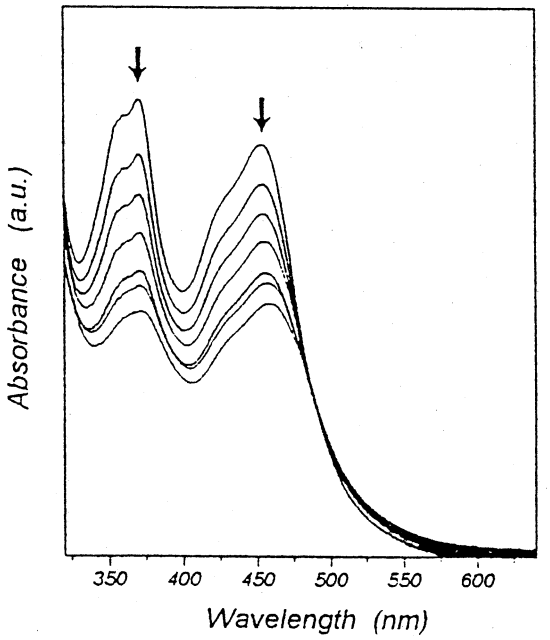

Fig. 5. The visible absorption spectra of $[Ru(ip)_2(dppz)]^{2+}$ (40 μM) in 5 mM Tris–HCl, 50 mM NaCl buffer (pH 7.0) in the presence of 0, 7, 14, 21,28, 32 and 42 μM calf thymus DNA.

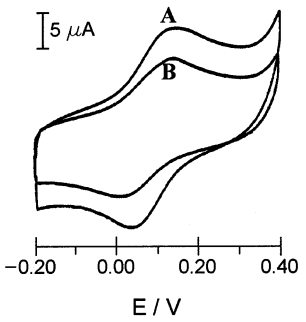

Fig. 6. Cyclic voltammograms of $[Co(phen)_2(ip)]^{3+}$ in the: (A) absence; and (B) presence of DNA in 50 mM NaCl, 10 mM Tris, pH 7.2. [Co] = 100 μM, [DNA]/[Co] = 20, scan rate 200 mV s^{-1}.

tive metal ion, Co(III) complexes provide a valuable chance to probe the DNA binding by electrochemical means and can find application in site specific DNA cleavage.

$[Co(phen)_2(ip)]^{3+}$ and $[Co(phen)_2(pip)]^{3+}$ were found to be bound intercalatively to DNA by using various photophysical and hydrodynamic methods [36], similar to their Ru(II) parent complexes [22]. The cyclic voltammograms of $[Co(phen)_2(ip)]^{3+}$

in the absence and presence of CT-DNA are shown in Fig. 6 and the electrochemical data are summarized in Table 2. Both $[Co(phen)_2(ip)]^{3+}$ and $[Co(phen)_2(pip)]^{3+}$ showed a pronounced decrease of the peak currents and shifts in $E_{1/2}$ to less negative potential upon addition of DNA. $[Co(phen)_2(pip)]^{3+}$ produced a more significant decrease in peak currents and shows a larger shift in $E_{1/2}$ upon binding to DNA. The drop of voltammetric currents in the presence of DNA can be attributed to diffusion of the metal complex bound to the large, slowly diffusing DNA molecule [33,37]. The more pronounced changes produced on addition of DNA in the voltammogram support the view that $[Co(phen)_2(pip)]^{3+}$ is bound to DNA more tightly than $[Co(phen)_2(ip)]^{3+}$ is.

It is not unexpected that, with a more extended aromatic ligand, the four Co(III) complexes $[Co(phen)_2(ip)]^{3+}$, $[Co(phen)_2(pip)]^{3+}$, [36] $[Co(bpy)_2(TATP)]^{3+}$ and $[Co(phen)_2(TATP)]^{3+}$ [38] show a higher DNA cleavage efficiency than that of $[Co(bpy)_3]^{3+}$ and $[Co(phen)_3]^{3+}$. Fig. 7 shows the gel electrophoretic separations of plasmid pBR322 DNA after incubation with $[Co(bpy)_2(TATP)]^{3+}$ and $[Co(phen)_2(TATP)]^{3+}$ and irradiation at 302 nm. $[Co(bpy)_2(TATP)]^{3+}$ and $[Co(phen)_2(TATP)]^{3+}$ cleave DNA to a much larger extent than $[Co(bpy)_3]^{3+}$ and $[Co(phen)_3]^{3+}$.

The observations mentioned above demonstrate that the electrochemical and photochemical results obtained from Co(III) complexes parallel very well their Ru(II) parent complexes [22,39].

Table 2
Voltammetric behavior of $[Co(phen)_2(ip)]^{3+}$ and $[Co(phen)_2(pip)]^{3+}$ bound to calf thymus DNA

Complex	R[a]	E_{pc} (V)	E_{pa} (V)	$E_{1/2}$ (V)
$[Co(phen)_2(ip)]^{3+}$	0	0.04	0.15	0.095
	40	0.026	0.13	0.078
$[Co(phen)_2(pip)]^{3+}$	0	−0.05	0.08	0.015
	40	−0.09	0.026	−0.032

[a] R is the ratio of the concentration of the cobalt complex to that of DNA.

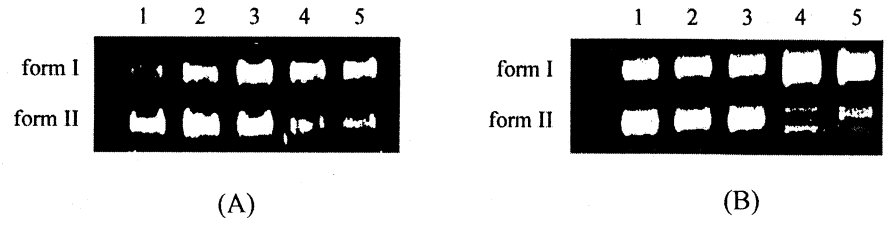

Fig. 7. (A) Cleavage of pBR322 DNA in the presence of $[Co(phen)_2(TATP)]^{3+}$ and light. The 0.8% agarose gel shows that the distribution of DNA forms initially without Co^{3+} (lane 1) and after irradiation at 302 nm in the presence of $[Co(phen)_2(TATP)]^{3+}$ for 0, 10, 20 and 30 mm (lane 2–5, from left to right). (B) Photoactivated cleavage of pBR322 DNA after 40 min irradiation at 302 nm with 1 (no complex), 2 ($[Co(bpy)_3]^{3+}$), 3 ($[Co(phen)_3]^{3+}$), 4 ($[Co(bpy)_2(TATP)]^{3+}$) and 5 ($[Co(phen)_2(TATP)]^{3+}$) [38]. Reproduced from ref. [38] with permissino of Elsevier Science.

3. Enantioselective binding to DNA

Enantioselective binding to DNA of the octahedral polypyridine complexes is a very interesting observation during the study on the interactions of this kind of complex with DNA. The first enantioselective binding model was established for $[M(phen)_3]^{n+}$ (M is Ru when $n=2$ and M is Co when $n=3$) by Barton [5]. The complex can insert one of its phenanthrolines into the DNA base pairs and the other two ligands remained in the DNA groove. The Δ enantiomer, a right-handed propeller-like structure, displays a greater affinity than the Δ enantiomer for right-handed CT-DNA, due to appropriate steric matching. Enantioselectivity was observed for many octahedral complexes upon binding to DNA by different techniques [9,13,15,40–43]. Furthermore, the enantioselectivity was reported to correlate well to the steric bulk of the ancillary ligands [40,44,45]. In our most recent work it was found that the enantioselectivity is also related distinctly to the shape of the intercalative ligand of the complex.

The DNA binding properties of complexes $[Ru(bpy)_2(HPIP)]^{2+}$, $[Ru(bpy)_2(HNOIP)]^{2+}$ and $[Ru(bpy)_2(HNAIP)]^{2+}$ were investigated by photophysical and hydrodynamic methods [46,47]. $[Ru(bpy)_2(HPIP)]^{2+}$ and $[Ru(bpy)_2(HNOIP)]^{2+}$ were found to be bound to DNA by intercalation while $[Ru(bpy)_2(HNAIP)]^{2+}$ may be a groove binder. To probe the enantioselectivity on binding to DNA in detail, these complexes were resolved into the pure enantiomer [18] by a well-documented method [48–52]. (Fig. 8) Each enantiomer was characterized systematically. The absolute configuration of the enantiomer was assigned ambiguously by applying excitation theory [53,54] and comparing with similar complexes of known configuration [50,55].

3.1. Electronic absorption spectra

For the three complexes above, the binding of the Δ and Λ isomers to CT-DNA led to hypochromism in the MLCT energy band and/or the IL band of the intercalating ligand in the visible region. The progressive decrease of intensity of the absorption spectra in the visible region for $[Ru(bpy)_2(HNOIP)]^{2+}$ and $[Ru(bpy)_2(HNAIP)]^{2+}$ on addition of CT-DNA is shown in Fig. 9. Some of the spectroscopic changes for the isomers bound to DNA are summarized in Table 3. As indicated by the results, the enantiomers of $[Ru(bpy)_2(HPIP)]^{2+}$ and $[Ru(bpy)_2(HNOIP)]^{2+}$ show more significant hypochromism than the enantiomers of $[Ru(bpy)_2(HNAIP)]^{2+}$. This may indicate that $[Ru(bpy)_2(HPIP)]^{2+}$ and $[Ru(bpy)_2(HNOIP)]^{2+}$ were bound to DNA more tightly than was $[Ru(bpy)_2(HNAIP)]^{2+}$. In addition, the difference in variation of the absorption spectra between the Δ and Λ isomers of $[Ru(bpy)_2(HNAIP)]^{2+}$ was somewhat larger than that between the individual isomers of $[Ru(bpy)_2(HPIP)]^{2+}$ and $[Ru(bpy)_2(HNOIP)]^{2+}$. This observation implies that the difference of binding geometry for the two enantiomeric isomers of $[Ru(bpy)_2(HNAIP)]^{2+}$ may be consistently larger.

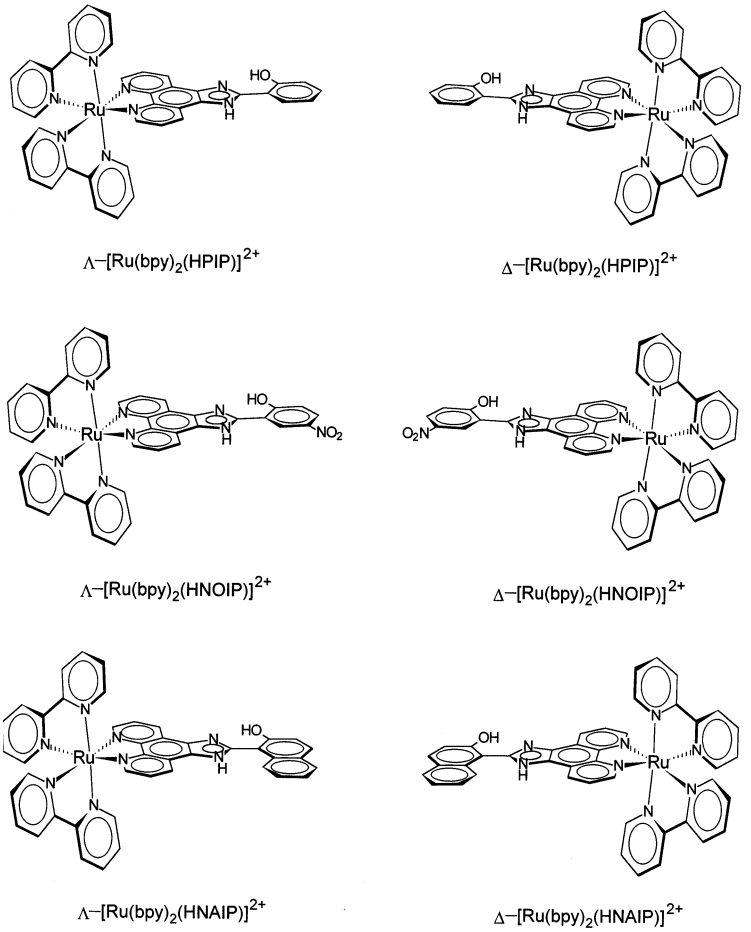

Fig. 8. Schematic illustrations of the Δ- and Λ- enantiomers of $[Ru(bpy)_2(HPIP)]^{2+}$, $[Ru(bpy)_2(HNAIP)]^{2+}$ and $[Ru(bpy)_2(HNOIP)]^{2+}$.

3.2. Steady-state emission titration

The results of the emission titration for the enantiomers of $[Ru(bpy)_2(HPIP)]^{2+}$ and $[Ru(bpy)_2(HNOIP)]^{2+}$ are illustrated with the titration curves in Fig. 10. The emission intensity of the isomers of $[Ru(bpy)_2(HPIP)]^{2+}$ in Tris buffer increased much more significantly than for the isomers of $[Ru(bpy)_2(HNAIP)]^{2+}$. Moreover, the difference in emission variation between the Δ and Λ isomers of $[Ru(bpy)_2(HNAIP)]^{2+}$ is larger than that of $[Ru(bpy)_2(HPIP)]^{2+}$ and $[Ru(bpy)_2(HNOIP)]^{2+}$. These results are consistent with the conclusions from the absorption spectra. $[Ru(bpy)_2(HNOIP)]^{2+}$ does not luminesce in Tris buffer but shows emission enhancement with increasing amounts of CT-DNA, which is similar to what is observed for $[Ru(bpy)_2(dppz)]^{2+}$ [31]. This effect has been called a

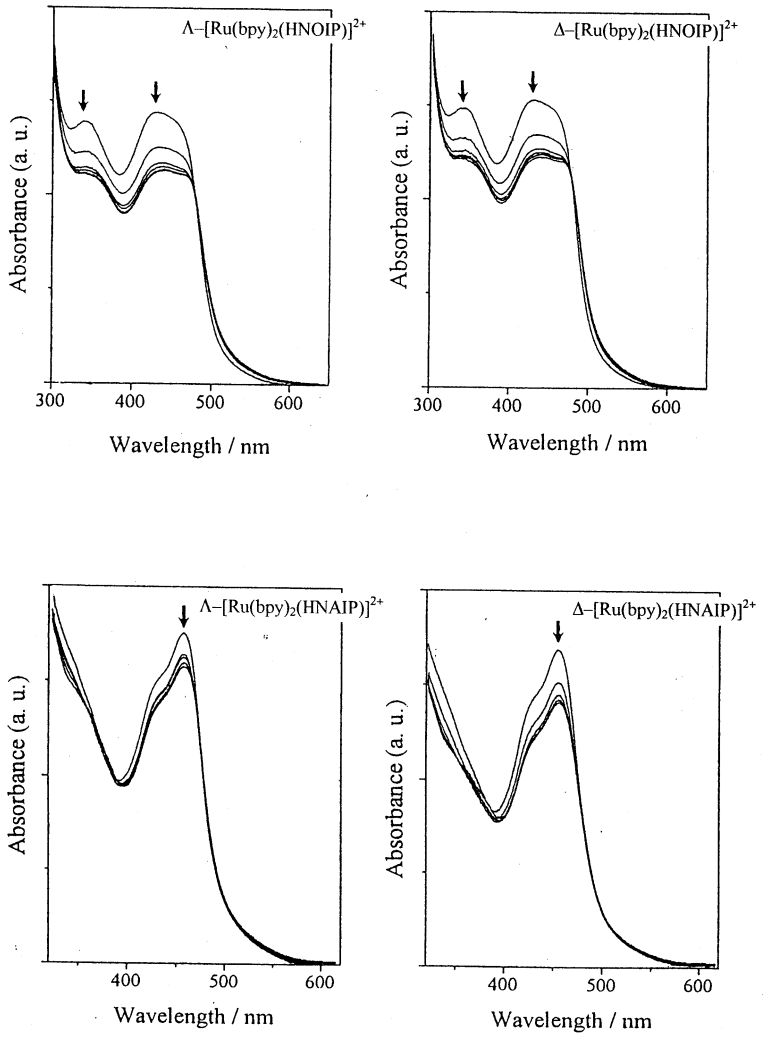

Fig. 9. Absorption spectra of and Δ- and Λ-$[Ru(bpy)_2(HNAIP)]^{2+}$, Δ- and Λ-$[Ru(bpy)_2(HNOIP)]^{2+}$ in 5 mM Tris–HCl and 50 mM NaCl (pH 7.2) in the absence and presence of increasing amounts of CT-DNA ([Ru] = 20 μM, [DNA] = 0–200 μM).

molecular "light switch" for DNA. However, it is noted that there is no significant difference in the emission behavior between Δ- and Λ-$[Ru(bpy)_2(HNOIP)]^{2+}$ upon DNA binding, which implies that the binding geometry of the two enantiomeric isomers may be very similar, as will be evident in equilibrium dialysis experiments.

Table 3
Electronic absorption spectra upon addition of CT-DNA

Complex	Absorption λ_{max} (nm)		Bathochromism $\Delta\lambda$ (nm)	Hypochromism%
	Free	Bound		
Δ-$[Ru(bpy)_2(HPIP)]^{2+}$	458	464	6	24.5
Λ-$[Ru(bpy)_2(HPIP)]^{2+}$	458	464	6	21.1
Δ-$[Ru(bpy)_2(HNAIP)]^{2+}$	456	458	2	15.3
Λ-$[Ru(bpy)_2(HNAIP)]^{2+}$	456	458	2	10.6
Δ-$[Ru(bpy)_2(HNOIP)]^{2+}$	434	442	8	23.4
	350	354	4	20.8
Λ-$[Ru(bpy)_2(HNOIP)]^{2+}$	434	442	8	22.1
	350	354	4	19.7

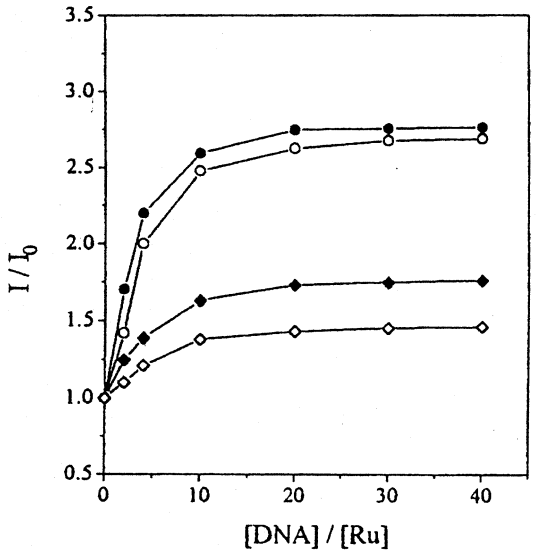

Fig. 10. Plots of relative emission intensity versus [DNA]/[Ru] ratio for Δ-$[Ru(bpy)_2(HPIP)]^{2+}$ (●) and Λ- $[Ru(bpy)_2(HPIP)]^{2+}$ (○), Δ-$[Ru(bpy)_2(HNAIP)]^{2+}$ (◆) and Λ-$[Ru(bpy)_2(HNAIP)]^{2+}$ (◇) [18]. Reproduced from ref. [18] with permission of Springer-Verlag.

3.3. Viscosity measurements

Compared with the above spectroscopic methods, hydrodynamic measurements that are sensitive to an increase in length (i.e. viscosity, sedimentation) are regarded as the least ambiguous and the most critical tests of a binding model in solution. As seen from Fig. 11, the viscosity of the DNA was increased by each set of isomers of $[Ru(bpy)_2(HPIP)]^{2+}$ and $[Ru(bpy)_2(HNOIP)]^{2+}$, but no noticeable difference

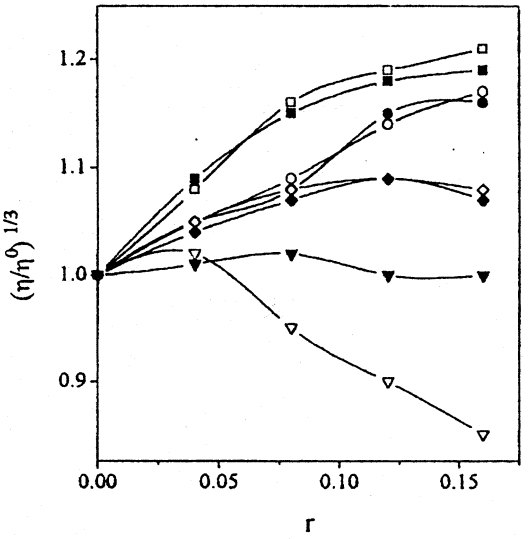

Fig. 11. Effects of increasing amounts of Δ-$[Ru(bpy)_2(HPIP)]^{2+}$ (○) and Λ-$[Ru(bpy)_2(HPIP)]^{2+}$ (●), Δ-$[Ru(bpy)_2(HNAIP)]^{2+}$ (▽) and Λ-$[Ru(bpy)_2(HNAIP)]^{2+}$ (▼), Δ-$[Ru(bpy)_2(HNOIP)]^{2+}$ (◇) and Λ-$[Ru(bpy)_2(HNOIP)]^{2+}$ (◆), and Δ-$[Ru(bpy)_2(dppz)]^{2+}$ (□) and Λ-$[Ru(bpy)_2(dppz)]^{2+}$ (■) on the relative viscosities of CT-DNA at 28.0(±0.1)°C. [DNA] = 0.5 mM and r = [Ru]/[DNA] [18]. Reproduced from ref. [18] with permission of Springer-Verlag.

was found. A surprising difference was observed between the two isomers of $[Ru(bpy)_2(HNAIP)]^{2+}$. The DNA viscosity is not appreciably affected by Δ-$[Ru(bpy)_2(HNAIP)]^{2+}$, but Λ-$[Ru(bpy)_2(HNAIP)]^{2+}$ decreases the viscosity. This effect had also been observed for the enantiomers of $[Ru(phen)_3]^{2+}$, for which the Δ isomer was proposed to intercalate partially into the DNA base pairs, while the Λ isomer may bind in the groove non-intercalatively [10].

3.4. Equilibrium dialysis

The equilibrium dialysis experiment may be one of the most direct means of examining the enantioselectivity of the complex upon binding to DNA [6]. Racemic solutions of the three complexes were dialyzed against CT-DNA with stirring for 48 h, and the dialysate was then subjected to circular dichroism analysis. Unexpectedly, the dialysate of $[Ru(bpy)_2(HNAIP)]^{2+}$ showed prominent CD signals with a positive peak around 275 nm and a negative peak around 295 nm, but there were no significant CD signals for the dialysate of $[Ru(bpy)_2(HPIP)]^{2+}$ and $[Ru(bpy)_2(HNOIP)]^{2+}$ (Fig. 12). The absence of CD signals for the two latter complexes is difficult to understand with respect to the results obtained from the spectroscopic experiments.

These observations prompted us to explore further with CD spectra the dialysis process for $[Ru(bpy)_2(HPIP)]^{2+}$ and $[Ru(bpy)_2(HNOIP)]^{2+}$ at varying time inter-

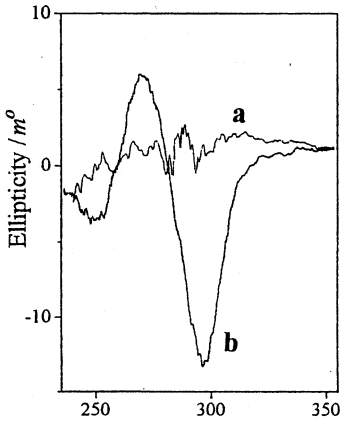

Fig. 12. CD spectra of the dialysate of $[Ru(bpy)_2(HPIP)]^{2+}$ (curve a) and $[Ru(bpy)_2(HNAIP)]^{2+}$ (curve b) after 48 h dialysis against CT-DNA with the solution stirred ([Ru] = 50 μM, [DNA] = 1.0 mM) [18]. Reproduced from ref. [18] with permission of Springer-Verlag.

vals. Fig. 13 shows the CD signals of the dialysate of $[Ru(bpy)_2(HPIP)]^{2+}$ varying with the dialysis time. From 0 to 26 h, the CD signal increases from zero to the maximum, then the signal begins to decrease and disappears after 48 h. For $[Ru(bpy)_2(HNOIP)]^{2+}$ no CD signal appears at all. This interesting result suggests that the equilibrium rates of the two enantiomeric isomers of $[Ru(bpy)_2(HPIP)]^{2+}$ are actually different upon being dialyzed against DNA. The appearance and disappearance of the CD signal of the Λ isomer indicates that Λ-$[Ru(bpy)_2(HPIP)]^{2+}$ equilibrates with DNA more rapidly than does Δ-$[Ru(bpy)_2(HPIP)]^{2+}$. A possible explanation for such an effect may be the difference in DNA binding geometry, and therefore binding affinity, for the Δ and Λ isomers of $[Ru(bpy)_2(HPIP)]^{2+}$ [18]. Different binding geometries have been utilized to explain the enantioselectivity of $[Ru(phen)_2(dppz)]^{2+}$ upon binding to DNA. Barton and coworkers proposed two binding modes: one is head-on intercalation and the other is side-on intercalation for $[Ru(phen)_2(dppz)]^{2+}$ on the basis of emission and NMR results [56–58]. Nordén and coworkers [42] suggest that the diastereomeric orientation effects of the chromophore and the different penetrations may be responsible for the enantiomeric selection based on LD. In our case the difference in emission perturbations between the Δ and Λ isomers of $[Ru(bpy)_2(HPIP)]^{2+}$ is not so large as that of the isomers of $[Ru(phen)_2(dppz)]^{2+}$, and we speculate that the different DNA binding behavior of Δ- and Λ-$[Ru(bpy)_2(HPIP)]^{2+}$ may have an explanation similar to the proposal of Nordén.

It is surprising that for the dialysate of $[Ru(bpy)_2(HPIP)]^{2+}$ the CD signal exhibited is assigned to the Δ form when compared with the CD spectrum of Δ-$[Ru(bpy)_2(HPIP)]^{2+}$, which means that the Λ isomer is favored for DNA binding. This is in contrast to the spectroscopic results. There is a clear trend for more significant changes in the absorption and emission spectra for the DNA-bound Δ-$[Ru(bpy)_2(HPIP)]^{2+}$. Such behavior is unusual, but it is not unprece-

dented. A similar ruthenium complex, $[Ru(bpy)_2(ppz)]^{2+}$ (ppz = 4′,7′-phenanthrolino-5′,6′:2,3-pyrazine) displayed the Δ CD signal in the dialysate upon dialysis against CT-DNA [16,17]. Since enantioselectivity is governed by many factors such as the DNA binding modes, the DNA sequence and the length of the duplex [15,30], further experiments using different probes and DNAs will contribute to a

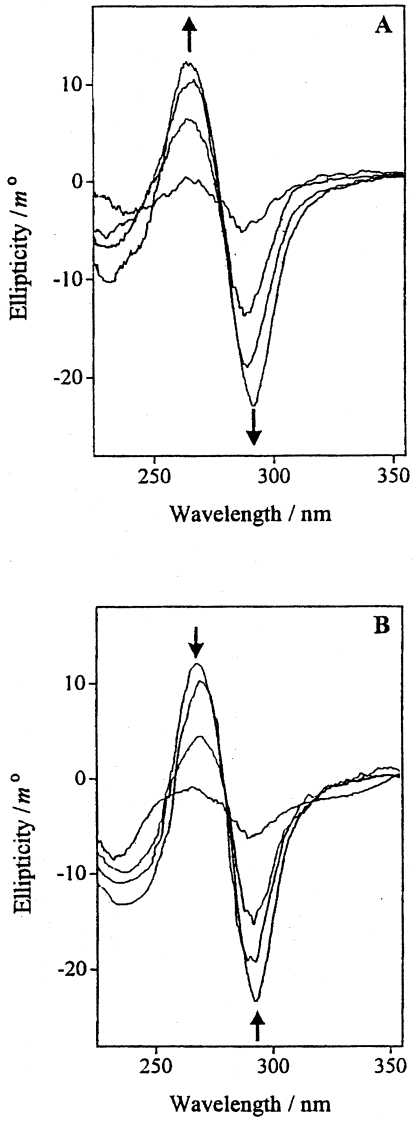

Fig. 13. CD spectra of the dialysate of $[Ru(bpy)_2(HPIP)]^{2+}$ after dialysis against CT-DNA for: (A) 6, 14, 20 and 26 h; and (B) 26, 32, 38 and 44 h with the solution stirred ([Ru] = 50 μM, [DNA] = 1.0 mM) [18]. Reproduced from ref. [18] with permission of Springer-Verlag.

complete understanding of enantiomeric selection. It should also be noted that the results from absorption, emission and CD spectra are an overall enantiomeric effect; other techniques including LD and NMR may provide detailed information on the DNA binding of enantiomeric isomers.

4. The further development of a molecular light switch for DNA

Polypyridyl complexes of ruthenium(II) can provide sensitive luminescent probes for double strand DNA in solution. Nevertheless, the background luminescence of the free complex in aqueous solution and their relatively weak binding constants appeared insufficient for their broad application as general non-radioactive nucleic acid probes. $[Ru(bpy)_2(dppz)]^{2+}$ and $[Ru(phen)_2(dppz)]^{2+}$, the most extensively investigated molecular light switches for DNA, exhibit a negligible background emission in water but luminesce intensely in the presence of double strand DNA with a high binding affinity ($K > 10^6\ M^{-1}$) [24,31,57]. This stimulated us to further develop novel light switches for DNA with a higher efficiency, based on the ruthenium(II) complex.

4.1. The design of novel molecular light switches for DNA

$[Ru(phen)_2(taptp)]^{2+}$ showed moderate hypochromism upon addition of CT-DNA with a red shift of 4 nm in the MLCT band, but it saturates quickly at a [DNA]/[Ru] ratio of 4.0 [59]. The binding constant of $6.4 \times 10^4\ M^{-1}$ was determined for the complex using the absorption at 465 nm. $[Ru(phen)_2(taptp)]^{2+}$ does not luminesce in water or in Tris buffer. The emission spectra of $[Ru(phen)_2(taptp)]^{2+}$ in Tris buffer at ambient temperature in the presence of increasing amounts of CT-DNA are shown in Fig. 14. Since $[Ru(phen)_2(taptp)]^{2+}$ and another

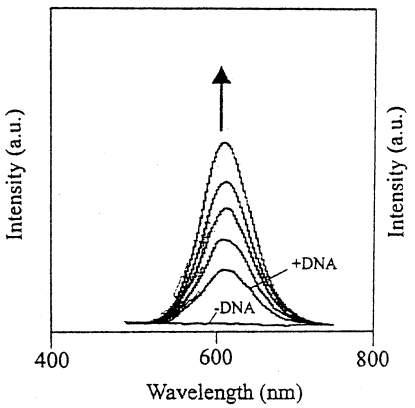

Fig. 14. Emission spectra of $[Ru(phen)_2(taptp)]^{2+}$ with increasing concentrations of calf thymus DNA: − DNA: in the absence of DNA; + DNA: in the presence of DNA [59]. Reproduced from ref. [59] with permission of Elsevier Science.

so-called light switch $[Ru(bpy)_2(tpphz)]^{2+}$ [60,61] are structurally analogous to $[Ru(phen)_2(dppz)]^{2+}$, it is instructive to compare their absorption and emission data upon binding to DNA — this is summarized in Table 4. It is clear that $[Ru(phen)_2(taptp)]^{2+}$ shows similar absorption changes to those of $[Ru(phen)_2(dppz)]^{2+}$. The quantum yield of $[Ru(phen)_2(taptp)]^{2+}$ is significantly lower than that of $[Ru(phen)_2(dppz)]^{2+}$, although the yield is somewhat higher than that of $[Ru(bpy)_2(tpphz)]^{2+}$. The dppz-based ligands taptp, tpphz and PHEHAT [62] are very similar in structure and their Ru(II) complexes exhibit light switch effects on DNA binding. It may be feasible to develop more efficient molecular light switches for DNA through modulation of the ligand dppz.

$[Ru(bpy)_2(HNOIP)]^{2+}$ [47], $[Ru(pztp)_2(phen)]^{2+}$ and $[Ru(pztp)_2(bpy)]^{2+}$ (pztp = 3-(pyrazin-2-yl)-as-triazino[5,6-f]1,10-phenanthroline) [63] are non-dppz based Ru(II) molecular light switches for DNA. $[Ru(bpy)_2(pip)]^{2+}$ and its derivatives bind intercalatively to CT-DNA with a relatively high binding affinity, but their strong background luminescence in the free form obscures the light switch effect [22,23,46]. Since the introduction of the nitro group to pip may quench the luminescence of the complex in aqueous solution [23], the novel complex $[Ru(bpy)_2(HNOIP)]^{2+}$ bearing hydroxyl and nitro was designed. Upon binding to DNA, $[Ru(bpy)_2(HNOIP)]^{2+}$ shows a slight AT sequence specificity. The maximum wavelength for emission shifts from 607 nm for the GC sequence to 615 nm for the AT sequence (Fig. 15).

As described before, $[Ru(bpy)_2(pztp)]^{2+}$ and $[Ru(phen)_2(pztp)]^{2+}$ do not luminesce either in the absence or presence of DNA [64]. To obtain greater insight into the effect of the pztp ligand on the emission behavior of the two complexes, two other related complexes $[Ru(pztp)_2(phen)]^{2+}$ and $[Ru(pztp)_2(bpy)]^{2+}$ were designed. The latter two complexes also do not luminesce in aqueous solution, but it is interesting that they luminesce at 590 nm and show emission enhancement in the presence of increasing amounts of CT-DNA upon excitation at 462 nm [63]. The results of emission titrations for $[Ru(pztp)_2(phen)]^{2+}$ and $[Ru(pztp)_2(bpy)]^{2+}$ with DNA are illustrated in Fig. 16. The typical relative intensities at the titration endpoints for $[Ru(pztp)_2(phen)]^{2+}$ and $[Ru(pztp)_2(bpy)]^{2+}$ are 0.07 and 0.35 using the emission of $[Ru(bpy)_3]^{2+}$ in Tris buffer as a standard. Fig. 16 indicates that the emission intensity of $[Ru(pztp)_2(bpy)]^{2+}$ grows much more quickly in comparison with $[Ru(pztp)_2(phen)]^{2+}$.

Table 4
Spectroscopic properties of $[Ru(phen)_2(taptp)]^{2+}$, $[Ru(bpy)_2(tpphz)]^{2+}$ and $[Ru(phen)_2(dppz)]^{2+}$ on binding to DNA

Complex	Emission		Absorption			
	I_{bound}	I_{rel} [a]	Free (nm)	Bound (nm)	$\Delta\lambda_{max}$ (nm)	Hypochromism (%)
$[Ru(phen)_2(taptp)]^{2+}$	613	0.33	465	469	4	8
$[Ru(bpy)_2(tpphz)]^{2+}$	622	0.24	444	440	4	23
$[Ru(phen)_2(dppz)]^{2+}$	618	0.56	439	439	0	12

[a] The value is presented as the intensity relative to that found for $[Ru(bpy)_3]^{2+}$ in H_2O.

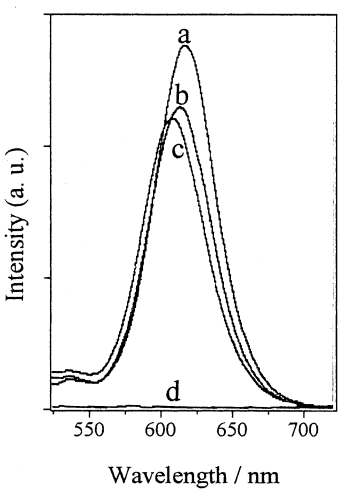

Fig. 15. Emission spectra of $[Ru(bpy)_2(HNOIP)]^{2+}$ (10 μM) in 5 mM Tris–HCl, 50 mM NaCl buffer (pH 7.0) at 298 K in the presence of (100 μM): (a) poly[dA]–poly[dT]; (b) calf thymus DNA; (c) poly[dG]–poly[dC]; and (d) absence of DNA.

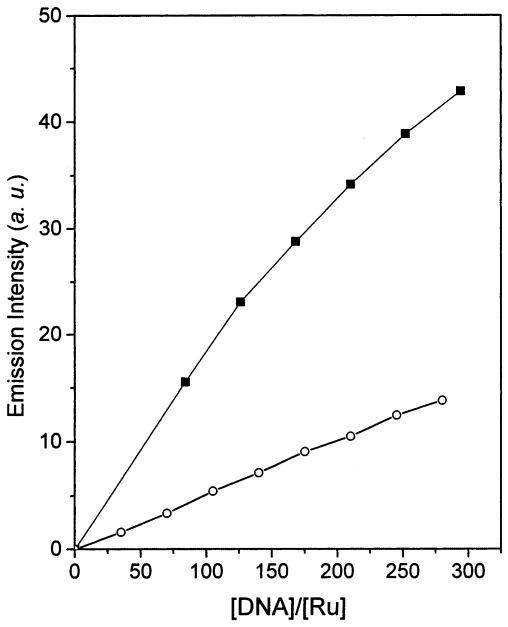

Fig. 16. Plots of emission intensity versus [DNA]/[Ru] ratio for $[Ru(pztp)_2(phen)]^{2+}$ (○) and $[Ru(pztp)_2(bpy)]^{2+}$ (■) [63]. Reproduced from ref. [63] with permission of Springer-Verlag.

4.2. Possible mechanism of the light switch effect for DNA

The mechanism of the light switch effect for $[Ru(phen)_2(dppz)]^{2+}$ has been studied intensively and the accumulated evidence points to hydrogen bonding and/or excited state proton transfer to the phenazine nitrogens as the mechanism of deactivation of the complexes' excited state [31,57,58,66–69].

To probe the possible mechanism involved in the light switch effect, the steady emission of $[Ru(phen)_2(taptp)]^{2+}$ [61] and $[Ru(bpy)_2(HNOIP)]^{2+}$ [47] in different media with varying polarities were explored [47,61]. The data are summarized in Table 5. The most interesting feature gathered from the data is that the polarity of the medium correlates well with its luminescence intensity: the more polar the solvent, the weaker is the emission. The absence of emission in H_2O for the two complexes may be explained on the basis of protonation of the nitrogen atoms in taptp and HNOIP. In addition, it is noted that the luminescence of $[Ru(pztp)_2(phen)]^{2+}$ and $[Ru(pztp)_2(bpy)]^{2+}$ in CH_3CN are very sensitive to water, being almost quenched completely in the presence of 5% water (v/v). Fig. 17(A) shows the progressive decrease of the emission intensity of $[Ru(pztp)_2(phen)]^{2+}$ in CH_3CN upon addition of H_2O. The titration curves showing the effect of H_2O on the emission of $[Ru(pztp)_2(phen)]^{2+}$ and $[Ru(pztp)_2(bpy)]^{2+}$ in CH_3CN are shown in Fig. 17(B). At low H_2O concentrations, ($[H_2O] < 0.3$ mol dm^{-3}), the data fit the Perrin sphere of quenching model very well. The Perrin sphere of quenching model assumes that the molecules are quenched completely if the quencher molecules are within a sphere of radius r, and that if any quenchers located outside this sphere they do not quench the emission at all [65]. A slope of 4.2 and a correlation coefficient (r) of 0.998 for $[Ru(pztp)_2(phen)]^{2+}$, and a slope of 7.2 ($r = 0.997$) for $[Ru(pztp)_2(bpy)]^{2+}$ were observed from Fig. 17(B). Based on Fig. 17(B), the luminescence of $[Ru(pztp)_2(bpy)]^{2+}$ is more sensitive to water than that of $[Ru(pztp)_2(phen)]^{2+}$. These results indicate that the above complexes may have a similar light switch mechanism to that proposed for $[Ru(phen)_2(dppz)]^{2+}$, whose emission is also solvent dependent and displays almost the same trend [69]. In our case the effect may be rationalized similarly in terms of the hydrophobic environment provided by DNA and the intercalative binding to DNA by the ligand

Table 5
Emission characteristics of $[Ru(phen)_2(taptp)]^{2+}$ and $[Ru(bpy)_2(HNIOP)]^{2+}$ in various solvents with different polarities

Complex	Solvent							
	CH_2Cl_2 (41.1)[a]		DMF (43.8)		CH_3CN (46)		H_2O (63.1)	
	I^{relb}	λ_{max}	I_{rel}	λ_{max}	I_{rel}	λ_{max}	I_{rel}	λ_{max}
$[Ru(phen)_2(taptp)]^{2+}$	1	598	0.66	614	0.26	617	0.0	–
$[Ru(bpy)_2(HNOIP)]^{2+}$	1	612	0.67	621	0.54	613	0.0	–

[a] The numbers given in kcal mol^{-1} in brackets are a measure of solvent polarity.
[b] The emission intensity I_{rel} is given as the ratio of the intensity in the solvent to that found in CH_2Cl_2.

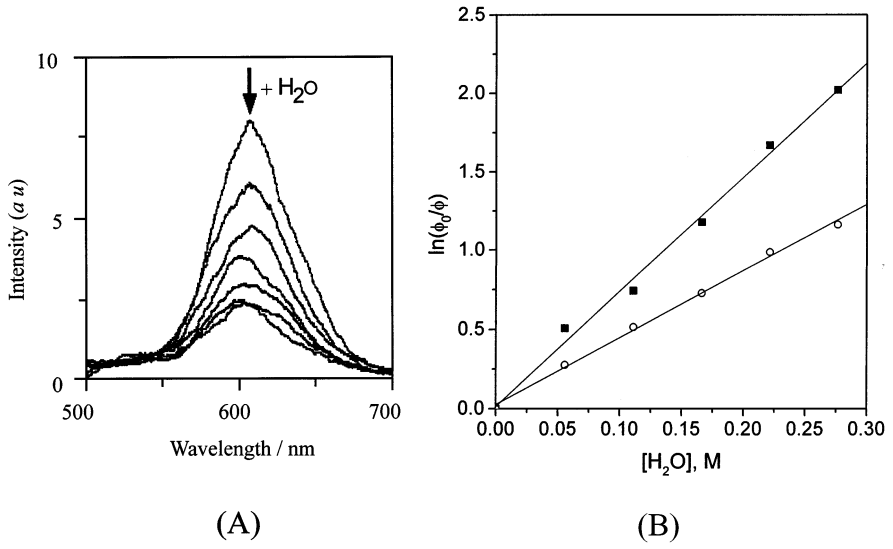

Fig. 17. (A) Emission spectra of $[Ru(pztp)_2(phen)]^{2+}$ in CH_3CN showing the change in intensity with increasing amount of H_2O ($[Ru] = 0.2$ mmol dm^{-3}, $[H_2O] = 0$–1.6 mol dm^{-3}). (B) Plots of $\ln(\phi_0/\phi)$ versus $[H_2O]$ for $[Ru(pztp)_2(phen)]^{2+}$ (○) and $[Ru(pztp)_2(bpy)]^{2+}$ (■) [63].Reproduced from ref. [63] with permission of Springer-Verlag.

HNOIP, taptp or pztp in our complexes, and a consequent protection of the ruthenium emission from quenching by water.

Acknowledgements

The authors are grateful to the National Natural Science Foundation of China, the State Key Laboratory of Bioorganic and Natural Products Chemistry in the Shanghai Institute of Organic Chemistry, the State Key Laboratory of Coordination Chemistry in Nanjing University and the Natural Science Foundation of Guangdong Province for their financial support. We also thank the following colleagues for their distinguished contributions to this research field: Y. Xiong, Q.X. Zhen, Q.L. Zhang, X.F. He, J.Z. Wu and L. Wang.

Appendix A. Abbreviations for ligands

bpy	2,2′-bipyridine
CIP	2-(2-chloro-phenyl-)imidazo[4,5-*f*]1,10-phenanthroline
dppz	dipyrido[3,2-*a*:2′3′-*c*]phenazine
DIP	4,7-diphenyl-1,10-phenanthroline
dptatp	2,3-diphenyl-1,4,8,9-tetraazatriphenylene

HPIP	2-(2-hydroxyphenyl-)imidazo[4,5-*f*]1,10-phenanthroline
HNAIP	2-(2-hydroxyl-1-naphthyl-)imidazo[4,5-*f*]1,10-phenanthroline
HNOIP	2-(2-hydroxy-5-nitro-phenyl-)imidazo[4,5-*f*]1,10-phenanthroline
ip	imidazo[4,5-*f*]1,10-phenanthroline
phen	1,10-phenanthroline
ppz	4′,7′-phenanthrolino-5′,6′:2,3-pyrazine
pip	2-phenyl-imidazo[4,5-*f*]1,10-phenanthroline
PHEHAT	1,10-phenanthrolino[5,6-*b*]1,4,5,8,9,12-hexaazatriphenlene
pztp	3-(pyrazin-2-yl)-*as*-triazino[5,6-*f*]1,10-phenanthroline
qpy	quaterpyridine
taptp	4,5,9,18-tetraazaphenanthreno[9,10-*b*]triphenylene
TATP	1,4,8,9-tetraazatriphenylene
tpphz	tetrapyrido[3,2-*a*:2′,3′-*c*:3″,2″-*h*:2″,3″-*j*]phenazine

Appendix B. Structural formulae of the ligands

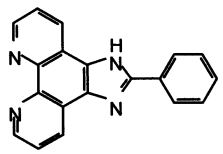
pip

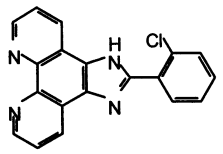
CIP

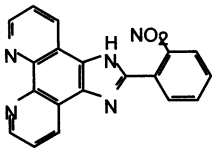
NIP

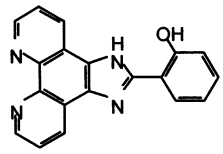
HPIP

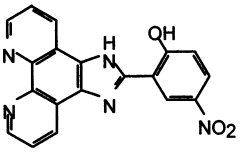
HNOIP

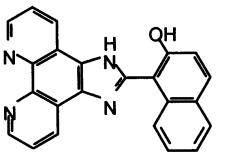
HNAIP

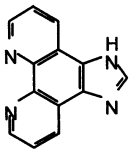
ip

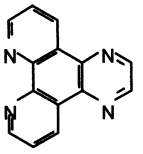
TATP

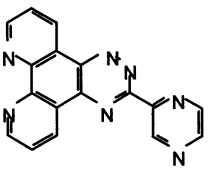
pztp

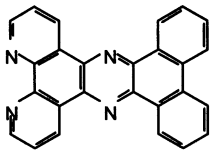
taptp

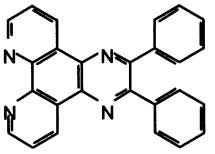
dptatp

References

[1] B. Nordén, P. Lincoln, B. Akerman, E. Tuite, in: A. Sigel, H. Sigel (Eds.), Metal Ions in Biological Systems, vol. 33, Marcel Decker, New York, 1996, pp. 177–252.
[2] R.E. Holmlin, P.J. Dandliker, J.K. Barton, Angew. Chem. Int. Ed. Engl. 36 (1997) 2714.
[3] C.J. Burrows, J.G. Muller, Chem. Rev. 98 (1998) 1109.
[4] A.M. Pyle, J.P. Rehmann, R. Meshoyrer, C.V. Kumar, N.J. Turro, J.K. Barton, J. Am. Chem. Soc. 111 (1989) 3051.
[5] J.K. Barton, Science 233 (1986) 727.
[6] J.K. Barton, A.T. Danishefsky, J.M. Goldberg, J. Am. Chem. Soc. 106 (1984) 2172.
[7] J.K. Barton, J.M. Goldberg, N.J. Turro, J. Am. Chem. Soc. 108 (1986) 2081.
[8] J.P. Rehmann, J.K. Baton, Biochemistry 29 (1990) 1701.
[9] C. Hiort, B. Nordén, A. Rodger, J. Am. Chem. Soc. 112 (1990) 1971.
[10] S. Satyanarayana, J.C. Dabrowiak, J.B. Chaires, Biochemistry 31 (1992) 9319.
[11] S. Satyanarayana, J.C. Dabrowiak, J.B. Chaires, Biochemistry 32 (1993) 2573.
[12] M. Eriksson, M. Leijon, C. Hiort, B. Nordén, A. Gräslund, J. Am. Chem. Soc. 114 (1992) 4933.
[13] M. Eriksson, M. Leijon, C. Hiort, B. Nordén, A. Gräslund, Biochemistry 33 (1994) 5031.
[14] J.E. Coury, J.R. Anderson, L. McFailisom, L.D. Williams, L.A. Bottomley, J. Am. Chem. Soc. 119 (1997) 3972.
[15] D.Z.M. Coggan, I.S. Haworth, P.J. Bates, A. Robinson, A. Rodger, Inorg. Chem. 38 (1999) 4486.
[16] R.J. Morgan, S. Chatterjee, A.D. Baker, T.C. Strekas, Inorg. Chem. 30 (1991) 2687.
[17] T.C. Strekas, A.D. Baker, L. Zaltsman, S.H. Wang, J. Coord. Chem. 39 (1996) 281.
[18] J.G. Liu, B.H. Ye, Q.L. Zhang, X.H. Zou, Q.X. Zhen, X. Tian, L.N. Ji, J. Biol. Inorg. Chem. 5 (2000) 119.
[19] L.S. Lerman, J. Mol. Biol. 3 (1961) 18.
[20] J.K. Barton, A.L. Raphael, J. Am. Chem. Soc. 106 (1984) 2466.
[21] C.V. Kumar, N.J. Turro, J.K. Barton, J. Am. Chem. Soc. 107 (1985) 5518.
[22] J.Z. Wu, B.H. Ye, L. Wang, L.N. Ji, J.Y. Zhou, R.H. Li, Z.Y. Zhou, J. Chem. Soc. Dalton Trans. (1997) 1395.
[23] Y. Xiong, X.F. He, X.H. Zou, J.Z. Wu, X.M. Chen, L.N. Ji, R.H. Li, J.Y. Zhou, K.B. Yu, J. Chem. Soc. Dalton Trans. (1999) 19.
[24] A.E. Friedman, C.V. Kumar, N.J. Turro, J.K. Barton, Nucleic Acids Res. 19 (1991) 2595.
[25] I. Haq, P. Lincoln, D. Suh, B. Nordén, B.Z. Chowdhry, J.B. Chaires, J. Am. Chem. Soc. 117 (1995) 4788.
[26] A.M. Pyle, J.K. Barton, in: S.J. Lippard (Ed.), Progress in Inorganic Chemistry: Bioinorganic Chemistry, vol. 38, Wiley, New York, 1990, pp. 413–475.
[27] Q.X. Zhen, B.H. Ye, Q.L. Zhang, J.G. Liu, H. Li, L.N. Ji, L. Wang, J. Inorg. Biochem. 76 (1999) 47.
[28] L. Wang, J.Z. Wu, G. Yang, T.X. Zeng, L.N. Ji, Transition Met. Chem. 21 (1996) 487.
[29] J.G. Liu, B.H. Ye, H. Li, L.N. Ji, R.H. Li, J.Y. Zhou, J. Inorg. Biochem. 73 (1999) 117.
[30] C. Hiort, P. Lincoln, B. Nordén, J. Am. Chem. Soc. 115 (1993) 3448.
[31] A.E. Friedman, J.-C. Chambron, J.-P. Sauvage, N.J. Turro, J.K. Barton, J. Am. Chem. Soc. 112 (1990) 4960.
[32] M.T. Carter, M. Rodriguez, A.J. Bard, J. Am. Chem. Soc. 111 (1989) 8901.
[33] M.T. Carter, A.J. Bard, J. Am. Chem. Soc. 109 (1987) 7528.
[34] S. Arounaguiri, B.G. Maiya, Inorg. Chem. 35 (1996) 4267.
[35] L. Jin, P. Yang, Polyhedron 16 (1997) 3395.
[36] Q.L. Zhang, J.G. Liu, H. Chao, L.N. Ji, Inorg. Biochem. in press.
[37] S. Mahadevan, M. Palaniandavar, Inorg. Chem. 37 (1998) 693.
[38] X.F. He, L. Wang, H. Chen, L. Xu, L.N. Ji, Polyhedron 17 (1998) 3161.
[39] L. Wang, PhD thesis, Zhongshan University, Guangzhou, 1996.
[40] T.P. Shields, J.K. Barton, Biochemistry 34 (1995) 15 049.
[41] C.M. Dupureur, J.K. Barton, Inorg. Chem. 36 (1997) 33.

[42] P. Lincoln, A. Broo, B. Nordén, J. Am. Chem. Soc. 118 (1996) 2644.
[43] K. Naing, M. Takahashi, M. Taniguchi, A. Yamagishi, Inorg. Chem. 34 (1995) 350.
[44] A. Sitlani, J.K. Barton, Biochemistry 33 (1994) 12 100.
[45] A. Sitlani, C.M. Dupureur, J.K. Barton, J. Am. Chem. Soc. 115 (1993) 12 589.
[46] J.G. Liu, B.H. Ye, H. Li, Q.X. Zhen, L.N. Ji, Y.H. Fu, J. Inorg. Biochem. 76 (1999) 265.
[47] J.G. Liu, B.H. Ye, H. Chao, Q.X. Zhen, L.N. Ji, Chem. Lett. (1999) 1085.
[48] X. Hua, A. von Zelewsky, Inorg. Chem. 34 (1995) 992.
[49] X. Hua, A. von Zelewsky, Inorg. Chem. 34 (1995) 5791.
[50] O. Morgan, S. Wang, S.A. Bae, R.J. Morgan, A.D. Baker, T.C. Strekas, R. Engel, J. Chem. Soc. Dalton Trans. (1997) 3733.
[51] F.R. Keene, Chem. Soc. Rev. 27 (1998) 185.
[52] D. Tzalis, Y. Tor, J. Am. Chem. Soc. 119 (1997) 852.
[53] B. Bosnich, Inorg. Chem. 7 (1968) 178.
[54] B. Bosnich, Inorg. Chem. 7 (1968) 2379.
[55] T.J. Rutherford, O.V. Gijte, A. Kirsch-De Mesmaeker, F.R. Keene, Inorg. Chem. 36 (1997) 4465.
[56] Y. Jenkins, A.E. Friedman, N.J. Turro, J.K. Barton, Biochemistry 31 (1992) 10 809.
[57] R.M. Hartshorn, J.K. Barton, J. Am. Chem. Soc. 114 (1992) 5919.
[58] Y. Jenkins, J.K. Barton, J. Am. Chem. Soc. 114 (1992) 8736.
[59] Q.X. Zhen, B.H. Ye, J.G. Liu, Q.L. Zhang, L.N. Ji, L. Wang, Inorg. Chim. Acta 303 (2000) 141.
[60] J. Bolger, A. Gourdon, E. Ishow, J. Launay, Inorg. Chem. 35 (1996) 2937.
[61] Q.X. Zhen, PhD thesis, Zhongshan University, Guangzhou, 1999.
[62] C. Moucheron, A. Kirsch-De Mesmaeker, S. Choua, Inorg. Chem. 36 (1997) 584.
[63] X.H. Zou, B.H. Ye, H. Li, Q.L. Zhang, H. Chao, J.G. Liu, L.N. Ji, Biol. Inorg. 6 (2001) 143.
[64] X.H. Zou, B.H. Ye, H. Li, J.G. Liu, Y. Xiong, L.N. Ji, J. Chem. Soc. Dalton Trans. (1999) 1423.
[65] N.J. Turro, Modern Molecular Photochemistry, Benjamin Cummings, Menlo Park, CA, 1978.
[66] C.M. Dupureur, J.K. Barton, J. Am. Chem. Soc. 116 (1994) 10 286.
[67] E.J. C. Olson, D. Hu, A. Hörmann, A.M. Jonkman, M.R. Arkin, E.D. A. Stemp, J.K. Barton, P.F. Babara, J. Am. Chem. Soc. 119 (1997) 11 458.
[68] C. Turro, S.H. Bossmann, Y. Jenkins, J.K. Barton, N.J. Turro, J. Am. Chem. Soc. 117 (1995) 9026.
[69] R.B. Nair, B.M. Cullum, C.J. Murphy, Inorg. Chem. 36 (1997) 962.